applied sciences

MDPI

Article

Fluoride Sorption Efficiency of Vermiculite Functionalised with Cationic Surfactant: Isotherm and Kinetics

Tayo Oladipo Ologundudu [1,*], John O. Odiyo [1] and Georges-Ivo E. Ekosse [2]

[1] Department of Hydrology and Water Resources, School of Environmental Sciences, University of Venda, P/Bag X5050, Thohoyandou 0950, South Africa; john.odiyo@univen.ac.za

[2] Directorate of Research and Innovation, University of Venda, P/Bag X5050, Thohoyandou 0950, South Africa; Georges-Ivo.Ekosse@univen.ac.za

* Correspondance: diposeg@yahoo.co.uk; Tel.: +27-83-239-2364

Academic Editor: Agustín Bueno-López
Received: 9 July 2016; Accepted: 15 September 2016; Published: 29 September 2016

Abstract: Groundwater is a major source of water, especially in rural communities. The presence of excess fluoride in groundwater has been a health concern for many decades because it causes fluorosis. The persistence of this problem led to the development of several approaches for reducing fluoride in groundwater to ≤1.5 mg/L, which is the World Health Organization's (WHO) permissible limit. Despite recorded success in fluoride reduction, drawbacks such as cost and efficiency have remained apparent, thus necessitating further research on defluoridation. This paper aims at assessing the defluoridation capacity of a clay mineral, vermiculite, when modified with the cationic surfactant hexadecyltrimethylammonium bromide. The effects of experimental parameters such as pH, agitation time, mass of adsorbent, and temperature were examined to determine the most favourable adsorption conditions. Using batch technique, the results showed a fluoride sorption of 51% from an 8 mg/L fluoride solution. The adsorption conformed more to Freundlich than Langmuir isotherm with an adsorption capacity of 2.36 mg/g, while the kinetics conformed to a pseudo-second-order reaction. pH emerged as the most influential factor in optimisation. The findings of this study indicated that modified vermiculite could be efficient in reducing fluoride in groundwater to more tolerable limits, but requires adequate pH control.

Keywords: adsorption; fluorosis; permissible limits; surfactant; vermiculite

1. Introduction

Groundwater is one of the major sources of water for domestic use especially in rural communities. Due to its source, groundwater contains several ions including sulphates (SO_4^{2-}), nitrates (NO_3^-), chlorides (Cl^-), carbonates (CO_3^{2-}), and phosphates (PO_3^{2-}), amongst others. These ions must remain within permissible limits to prevent negative impacts on human health. Fluoride, one of the impurities in groundwater has received much attention in recent times because of its health concerns. At low concentrations, fluoride is important to humans for the prevention of tooth decay, especially in children. However, excessive consumption of fluoride can lead to health complications such as dental, skeletal, and non-skeletal fluorosis [1]. Thus the World Health Organization (WHO) has specified the permissible limit of fluoride in potable water as 1.5 mg/L [2].

The occurrence of high fluoride in groundwater in particular has led to the development of defluoridation techniques based on the concepts of adsorption [3], precipitation [4], and membrane processes [5]. Adsorption is the most appropriate method because it has a combination of affordability and effectiveness [6].

Clay minerals such as montmorillonite [7], kaolinite [8], and bauxite [9] have been used as adsorbents for defluoridation. The effectiveness of these materials have been improved by modification processes such as acid treatment [8] and metal impregnation [10], amongst others. Vermiculite—one of the common clay minerals, which originates from the mica group—despite having its largest global deposit in the Phalaborwa area of Limpopo Province (South Africa), has not been exploited for its defluoridation potential. Thus this study sheds more light on the possible uses of this geological material. Vermiculite is generally composed of hydrous magnesium aluminium layers interpolated by layers of H_2O [11]. The structure is composed of two tetrahedral sheets attached to a central octahedral sheet, hence its structure is referred to as "2:1 phyllo-silicate" [12]. Al^{3+} substitution for Si^{4+} in the tetrahedral layers and Mg^{2+} or Fe^{2+} substitutions for Al^{3+} in the octahedral layers are responsible for the overall negative charge of the vermiculite structure [13]. This negative charge is balanced by the presence of exchangeable cations such as Na^+, K^+, Ca^{2+}, Mg^{2+}, and Al^{3+} within the interlayer spaces [14]. Besides the use of inorganic modifying agents, organic compounds, such as surfactants, have also been used to modify clay minerals to form organoclay.

An organoclay is a class of material formed when the exchangeable cations of a clay mineral are replaced by a quaternary ammonium cation (otherwise known as a surfactant) [15]. This process changes the overall surface charge of the clay mineral (i.e., vermiculite) from negative to positive, thus enhancing electrostatic attraction of negatively charged species in solution. Hexadecyltrimethylammonium bromide ($C_{19}H_{42}BrN$) is one such cationic surfactant used to prepare organoclays for adsorption purposes. Examples of such applications include the use of organosmectite for the removal of chromates from solution [16], organovermiculite for the removal of anionic dyes and herbicides from surface water [17,18], and organokaolinite for the removal of oxyanions from wastewater [19]. Though these studies have shown that organoclays have been effectively used for the removal of such anions from solutions, organoclays have not been actively used for the removal of fluoride from solution, thus this study explains more on the subject area. The efficiency of vermiculite functionalised with hexadecyltrimethylammonium bromide (HDTMABr) for fluoride sorption was evaluated in this study using higher concentrations of the surfactants. This approach is quite contrary to the conventional methods where surfactants concentrations equivalent to 50%, 100%, and 200% of the cation exchange capacity (CEC) are used for organoclay preparation. The mechanism of adsorption of anions on organomineral complexes is believed to be a strong electrostatic attraction [20] and chemical reduction of the anion on the surface of the adsorbent [21].

2. Materials and Methods

2.1. Materials

Superfine grade of vermiculite was obtained from Mandoval Vermiculite, Alberton, South Africa. The sample was milled and sieved to $\leq$250 µm using a mechanical sieve. All reagents used in this study were of analytical grade and were prepared using deionised water. The CEC of the vermiculite was analysed by the method described in Radojevic and Bashkin [22]. Sodium fluoride (NaF) stock solution of 1000 mg/L was prepared by dissolving 2.21 g of NaF salt in deionised water, and any subsequently required fluoride solutions were prepared by diluting the stock solution. The clay mineral was activated by agitating with 1 M sodium chloride (NaCl) in the ratio of 1:10 before modification, while silver nitrate ($AgNO_3$) was used to test the presence of any excess chloride after the activated clay was washed with deionised water. Hydrochloric acid (0.1 M HCl) and sodium hydroxide (0.1 M NaOH) were used to adjust the pH. Total ionic strength adjustment buffer (TISAB III) was used to remove the effect of complexing cations.

2.2. Preparation of Surfactant-Modified Vermiculite

Pretreatment of clay minerals with sodium enhances exchange of cations with the organic cation [23]. Vermiculite was first activated by agitating in 1 M NaCl in the ratio of 1:10 at room

temperature. The treated vermiculite was centrifuged and washed with deionised water until chloride was confirmed absent using $AgNO_3$ test. The Na-activated vermiculite was dried at 105 °C for 6 h and cooled in a desiccator. The CEC of vermiculite was determined to be 0.525 mmol/g, thus for 3 g of vermiculite, 1.575 mmol would be equivalent to 100% of the CEC. Subsequently 253.81% (0.2 M), 380.71% (0.3 M), and 507.61% (0.4 M) of the CEC was used for this analysis.

The homoionic clay of 3 g and deionised water was prepared in a 5% w/v solution, into which 20 mL of 0.2, 0.3, and 0.4 M HDTMABr was added and the solution was agitated for 24 h at 40 °C as carried out in Yu et al. [17]. The mixture was centrifuged and washed several times with deionised water to remove excess bromide. This was confirmed when no white precipitate was formed on addition of $AgNO_3$ to the washouts. The washed adsorbent was dried at 105 °C for 6–12 h and cooled in a desiccator. The adsorbents were labelled as HDTMA-$VMT_{0.2}$, HDTMA-$VMT_{0.3}$, and HDTMA-$VMT_{0.4}$, respectively.

2.3. Characterisation of Adsorbent

Characterisation techniques such as Fourier transform infrared (FTIR) and scanning electron microscopy (SEM) were used on both modified and fluoride-loaded adsorbents to understand the adsorbents as well as the properties that could be responsible for adsorption. The infrared spectrum of the adsorbent before and after defluoridation were captured using Alpha FTIR spectrometer (Bruker Optics, Billerica, MA, USA) in the range of 4000–400 cm^{-1}. The SEM characterisation was carried out using TESCAN, Vega 3XMU (TESCAN, Brno, Czech Republic).

2.4. Batch Adsorption Experiments

Batch equilibration technique was used for fluoride sorption experiments. A weighed quantity of each form of modified vermiculite (HDTMA-$VMT_{0.2}$, HDTMA-$VMT_{0.3}$, and HDTMA-$VMT_{0.4}$) was agitated with 10 mg/L fluoride solution at room temperature and 200 rpm, thus, the modification with the highest fluoride removal was used for the rest of analysis (optimisation). The optimisation was carried out in 250 mL shaking bottles containing 50 mL of 8 mg/L fluoride solution and a weighed quantity of the adsorbent. The effect of pH on the agitating mixture was investigated by varying from 2 to 10 while noting the pH with the most favourable fluoride removal. Other parameters which were investigated include: adsorbent dosage (0.1–2 g), contact time (5–70 min), adsorbate concentration (5–100 mg/L), and temperature (25 °C–55 °C). After each experiment, the test solution was centrifuged at 5000 rpm for 10 min and the supernatant decanted to a 100 mL beaker. To 10 mL of the decanted solution, 1 mL of TISAB (III) was added (10:1) to complex with any cation present and the residual fluoride was determined using an ion-selective electrode. The percentage fluoride removal was calculated using Equation (1).

$$\% \, Fluoride = \frac{C_o - C_e}{C_o} \times 100 \quad (1)$$

where C_o and C_e are the initial and equilibrium concentrations of the adsorbate (mg/L), respectively. The amount of fluoride (q_e) adsorbed in milligram per gram of the adsorbent was calculated using Equation (2).

$$q_e = \frac{C_o - C_e}{m} \times v \quad (2)$$

where m is the mass (g) of adsorbent and v is the volume of the solution in litres (L).

The adsorption isotherm was determined using the data obtained from optimisation of adsorbate concentration. The adsorption kinetics and mechanism-based model were, however, determined using data obtained from optimisation of contact time.

3. Results

3.1. Effect of HDTMA Strength

The effectiveness of the different forms of modification are plotted in Figure 1. The plot shows that the 0.2 M modification had the highest fluoride removal of 13.6%. This was so because the 0.2 M modified vermiculite contained the most electropositive surface (lowest solution pH). Thus HDTMA-$VMT_{0.2M}$ was used for the optimisation process after the pH of the adsorbent surface was reduced to 1.5 before drying. This was carried out to further enhance electrostatic attraction between the surface of the organoclay and the fluoride in the solution.

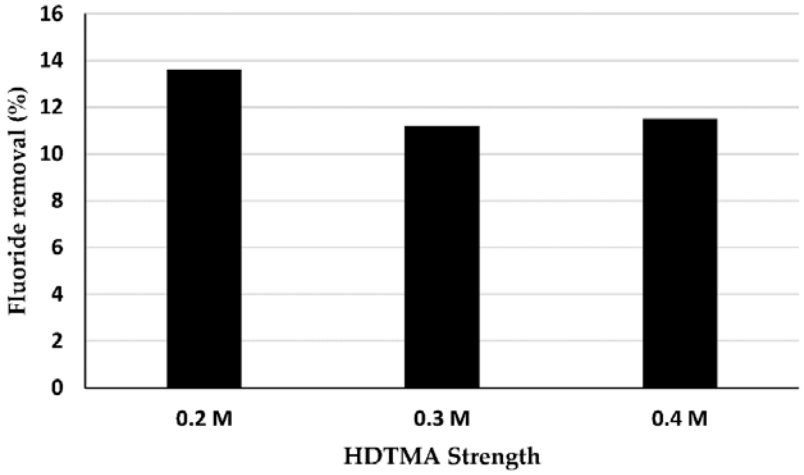

Figure 1. Plot of fluoride removal against hexadecyltrimethylammonium bromide (HDTMA) strength.

Hexadecyltrimethylammonium forms a monolayer or bilayer in the interlayer spaces of the vermiculite depending on the concentration used. Below the critical micelle concentration (CMC), HDTMA forms a monolayer (negative charge); however, above the CMC a bilayer is formed which is positively charged and enhances anionic sorption [24]. The CMC of HDTMA is 0.9 mM [25], thus a bilayer is formed when the high concentration of HDTMA was used in this study. This brings about a positive charge on the adsorbent surface which attracts fluoride from the solution. Figure 2 shows a diagram of the monolayer and bilayer arrangement of HDTMA on the interlayer spaces of vermiculite with fluoride attraction.

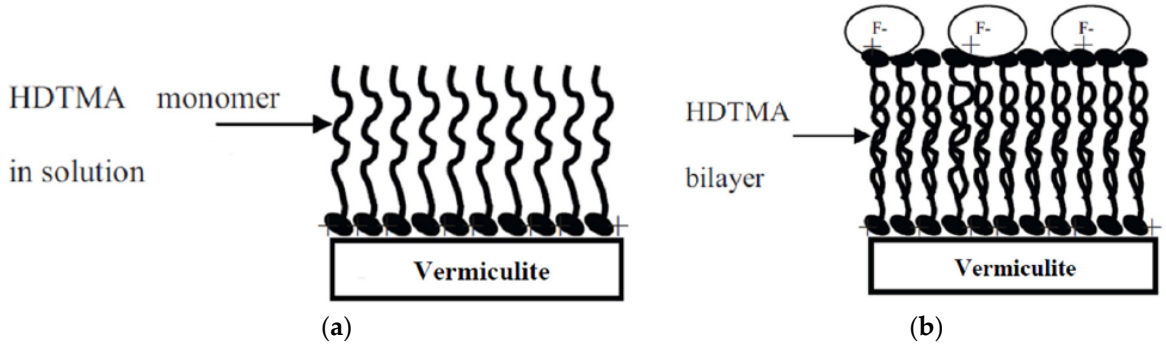

Figure 2. Monolayer (**a**) and bilayer (**b**) arrangement of HDTMA. Reproduced with permission from [26], Elsevier, 2012.

3.2. Fourier Transform Infrared

The FTIR analysis of HDTMA-$VMT_{0.2M}$ before and after defluoridation showed the functional groups of the adsorbent and identified regions of fluoride adsorption. Figure 3 shows the IR spectra of both stages.

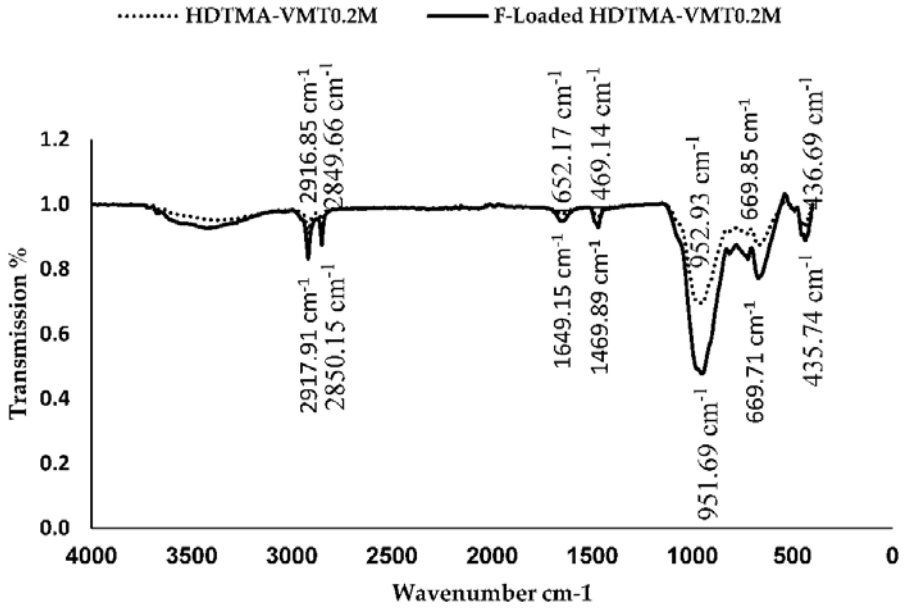

Figure 3. Fourier transform infrared (FTIR) analysis of HDTMA-$VMT_{0.2M}$ before and after defluoridation.

The spectra of HDTMA-$VMT_{0.2M}$ before and after defluoridation showed the major functional groups and established that fluoride sorption took place. Before defluoridation, the spectra showed a peak at 952.93 cm^{-1}, which corresponds to Si–O stretching vibrations of Si–O–Si silicate bonding [17]. The band at 1652.17 cm^{-1} represents O–H bending vibration of hydrating water molecules [27], while the bands at 669.85 and 436.69 cm^{-1} represent the Si–O bending modes [28]. More specifically, the spectrum of the HDTMA-$VMT_{0.2M}$ showed peculiar peaks at 2916.85 (CH_3), 2849.66 (CH_2), and 1469.14 (CH_3) cm^{-1}, which indicates the modification of vermiculite with HDTMA as observed in Yu et al. [17] and Slimani et al. [29].

A careful examination of the transmittance axis of HDTMA-$VMT_{0.2M}$ after defluoridation reveals a decrease in intensity of specific bands at 2917.91, 2850.15, 1469.89 cm^{-1}, and 951.69 cm^{-1}. The reduction to their new transmittance values suggested that the available sites created by the HDTMA (CH_3, CH_2) had been occupied by fluoride and is an indication of fluoride sorption [20].

3.3. Scanning Electron Microscopy

The micrographs before defluoridation reveal that the HDTMA-$VMT_{0.2M}$ appears flaky (Figure 4a). This observed morphology of HDTMA-$VMT_{0.2M}$ before defluoridation can be attributed to the effect of the modifying agent which brings together the particles of vermiculite into aggregates, thereby giving it a flaky structure as also observed by Muiambo [27]. After defluoridation, the HDTMA-$VMT_{0.2M}$ shows protuberances on its morphology owing to the addition of fluoride (Figure 4b).

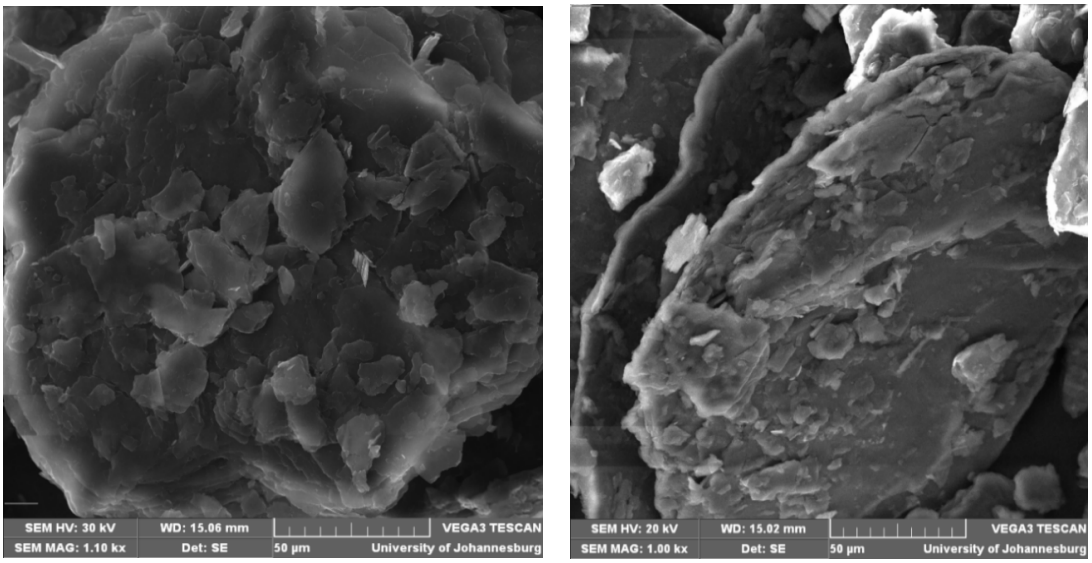

(**a**) (**b**)

Figure 4. SEM of HDTMA-VMT$_{0.2M}$ before (**a**) and after (**b**) fluoride sorption.

3.4. Optimisation of Experimental Parameters Using HDTMA-VMT$_{0.2M}$

3.4.1. Effect of Agitation Time

Figure 5 shows the plot of fluoride removal against time. The use of two different sorbent/water ratios established the reproducibility and consistency of the result. Contact time was consistent throughout the experiment with no significant change in fluoride removal from 5 to 60 min for both masses. At 70 min, fluoride removal increased consistently for both 0.2 and 0.4 g of HDTMA-VMT$_{0.2M}$ to give the maximum fluoride removal of 20.38% and 29.5%, respectively. The longest removal time observed in this series (contact time) of 70 min was maintained for subsequent experiments.

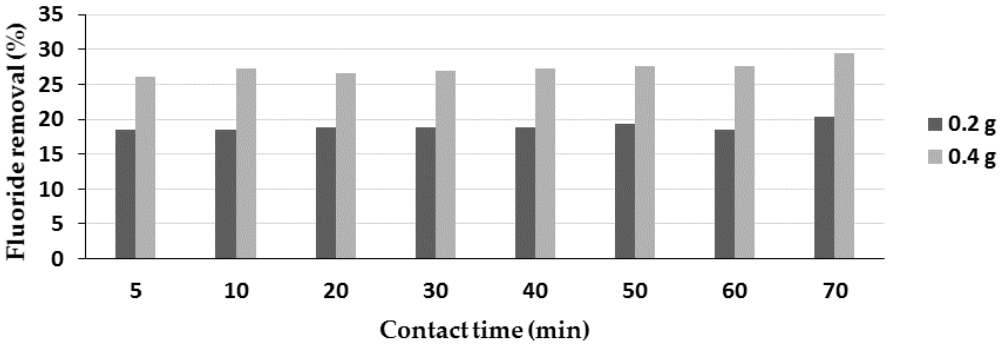

Figure 5. Optimisation of contact time (0.2 and 0.4 g/50 mL, 25 °C, 200 rpm).

3.4.2. Effect of Adsorbent Dosage

On increase of dosage of the adsorbent (0.2–2 g) with 50 mL of 8 mg/L fluoride solution, percentage fluoride removal increased steadily (Figure 6). Thus, increase in adsorbent dosage resulted in an increase in fluoride removal, as similarly observed in Dang-I et al. [30]. Based on the trend of the plot, further increase in adsorbent mass would have led to an improved fluoride removal due to availability of adsorbent sites. However, additional mass of HDTMA-VMT$_{0.2M}$ beyond 2 g caused bulkiness and near saturation of the adsorbent in the solution, which was not appropriate for defluoridation. The adsorbent mass of 2 g was therefore chosen as the optimum mass of HDTMA-VMT$_{0.2M}$ for subsequent fluoride removal trials.

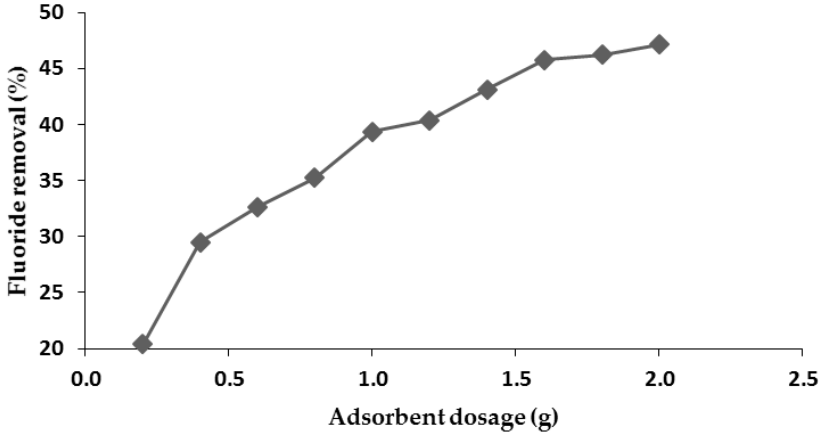

Figure 6. Optimisation of mass (70 min, 25 °C and 200 rpm).

3.4.3. Effect of Adsorbate Dosage

From Figure 7, the percentage fluoride removal decreased as the concentration of fluoride increased. This was due to the use of a constant mass of adsorbent while the adsorbate concentration increased, thus the adsorbent sites attained early saturation. Therefore, the higher the concentration of fluoride, the lower the defluoridation potential of HDTMA-$VMT_{0.2M}$. The adsorption capacity, however, increased as the concentration of adsorbate increased in the solution because the quantity of adsorbate in mg, which accumulated per gram of the adsorbent increased. This was consistent with findings by Thakre et al. [31] and Yilmaz et al. [32].

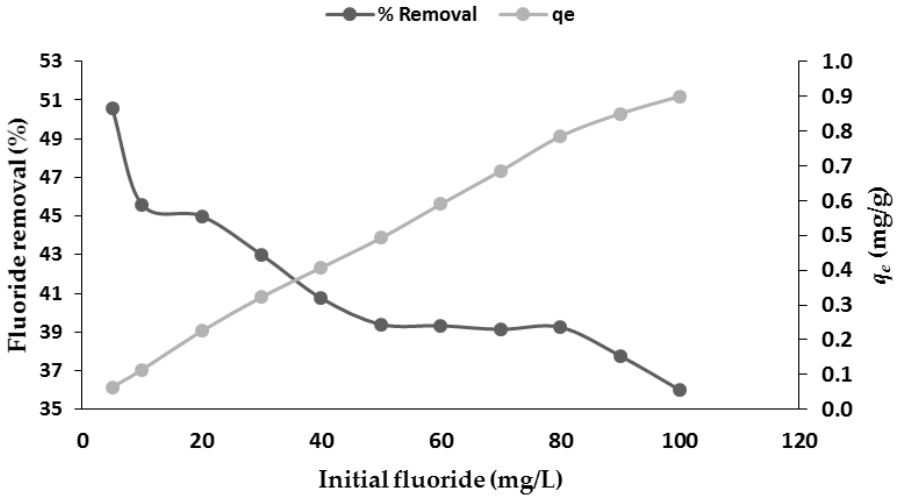

Figure 7. Fluoride removal and adsorption capacity against initial fluoride.

3.4.4. Effect of pH

The effect of pH on fluoride removal is plotted in Figure 8. The plot shows low fluoride removal at an acidic pH of 2, a peak removal at pH4 (51.13%), and a declining trend as the pH increases to 10. The fluoride removal was very low in acidic pH of 2 because the extremely high acidity triggered the formation of weak hydrofluoric acid, which prevented the adsorption of fluoride on the adsorbent [32–34]. An increase in pH beyond 6 led to a definite decline of adsorption as the surface of the adsorbent lost electropositivity and gained electronegativity, thereby creating a low force of attraction for fluoride. This negative media also creates competition between the fluoride and hydroxyl in solution, thus leading to reduced adsorption [32].

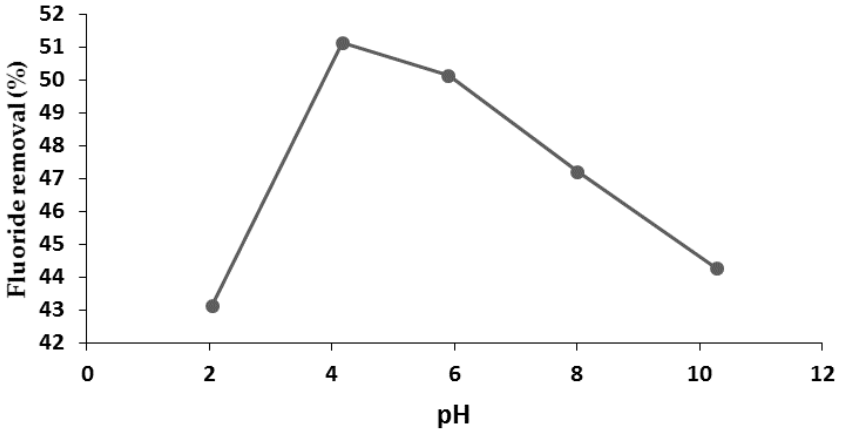

Figure 8. Optimisation of pH (2 g/50 mL, 70 min, 25 °C, 200 rpm).

3.4.5. Effect of Temperature

Investigation on the effect of temperature in this study showed that temperature has a negative effect on defluoridation. Figure 9 shows the results, and it can be seen that there is a gradual decline in percentage removal as the temperature increases. It was also observed that the equilibrium pH of the solution increased after shaking. Thus, increase in temperature increased the alkalinity of the solution, probably by removing the hydroxyl from the chemical formula of vermiculite ($M_x(Mg^{3+})(Si_{4-x}Al_x)O_{10}(OH)_2 \cdot nH_2O$). Room temperature (25 °C) therefore, is the most appropriate temperature for fluoride removal in this study.

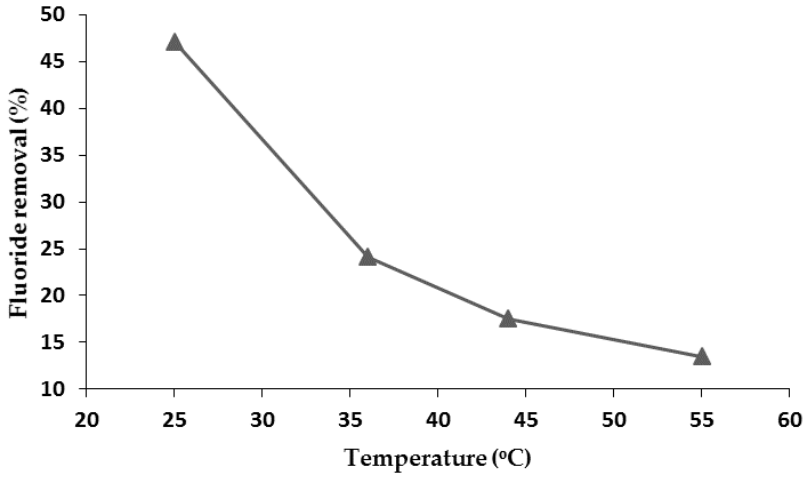

Figure 9. Optimisation of temperature (2 g/50 mL, 70 min, 200 rpm).

3.5. Adsorption Isotherm

The Langmuir isotherm describes quantitatively the formation of a monolayer of the adsorbate (fluoride) on smooth surface of the adsorbent (HDTMA-$VMT_{0.2M}$) [35]. After the surface of the adsorbent is completely occupied, no further adsorption of fluoride from solution takes place. The linear form of the Langmuir equation is represented by Equation (3).

$$\frac{C_e}{q_e} = \frac{C_e}{q_o} + \frac{1}{q_o K_L} \tag{3}$$

where C_e and q_e have been defined in Equations (1) and (2), q_o is the maximum monolayer coverage (mg/g), and K_L is Langmuir isotherm constant (L/mg).

A plot of C_e/q_e against C_e for this study gave a correlation coefficient of 0.8902 but did not give a linear plot (Figure 10). The adsorption capacity/maximum monolayer coverage was calculated from the slope to be 2.3669 mg/g (Table 1) and it can be inferred that only a degree of monolayer adsorption occurred on the surface of the adsorbent.

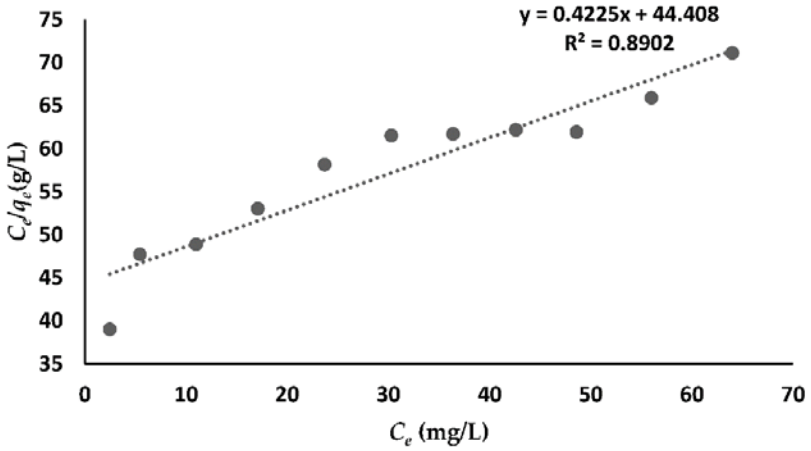

Figure 10. Langmuir isotherm plot of HDTMA-$VMT_{0.2M}$.

Table 1. Adsorption isotherm constants.

Adsorbent	Langmuir Isotherm				Freundlich Isotherm		
	q_o (mg/g)	K_L (L/mg)	R^2	R_L	K_L (L/mg)	1/n	R^2
HDTMA-$VMT_{0.2M}$	2.3669	0.0095	0.8902	0.9294	0.0293	0.8357	0.9985

The conformity of the adsorption to Langmuir isotherm was confirmed using Equation (4).

$$R_L = \frac{1}{(1 + bC_o)} \tag{4}$$

where R_L is the separation factor, C_o has been defined in Equation (1), and b is the Langmuir constant (L/mg). $R_L > 1$ represents an unfavourable monolayer adsorption, $R_L = 1$ represents a linear adsorption, $0 < R_L < 1$ represents a favourable adsorption process, and $R_L = 0$ represents an irreversible adsorption process [29]. The R_L value of this study was calculated to be 0.9294 (Table 1), thus monolayer adsorption took place which conforms to Langmuir isotherm.

The Freundlich isotherm models multilayer adsorption on heterogeneous surfaces. The Freundlich equation is formulated in Equation (5) as:

$$q_e = K_F C_e^{1/n} \tag{5}$$

where K_F is the constant of the system and is known as the Freundlich adsorption coefficient, n is the Freundlich constant, while the value of n should be between 1 and 10 for favourable adsorption [36]. By taking logarithm of Equation (5):

$$\log q_e = \log K_F + \frac{1}{n} \log C_e \tag{6}$$

A plot of $\log q_e$ against $\log C_e$ for this study gave a linear plot with a correlation coefficient of 0.9985 (Figure 11). This shows that the adsorption conformed more to Freundlich isotherm than Langmuir. The value of $1/n$ was also calculated to be 0.8357 (n = 1.1966), which implies an affinity between the surface of the adsorbent and fluoride [37]. The adsorption capacity of HDTMA-$VMT_{0.2M}$, though on the higher side, is approximately similar to the capacities of many other fluoride adsorbents reported in

literature as shown in Table 2. This can simply be attributed to a higher amount of adsorbate (fluoride) adsorbed per gram of HDTMA-VMT$_{0.2M}$ than the other adsorbents used for comparison in this study.

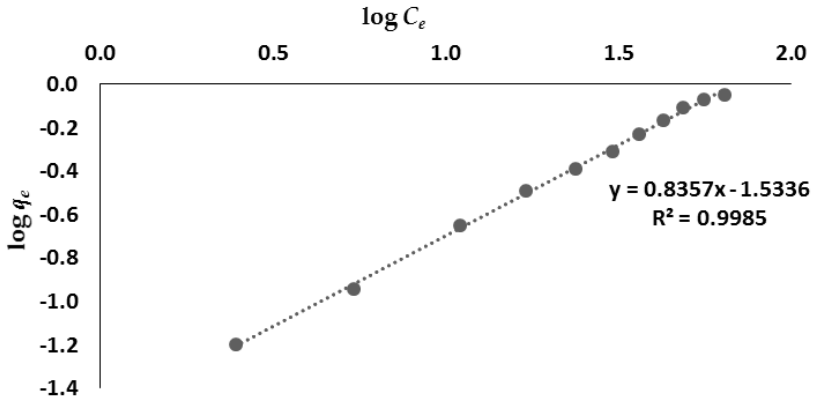

Figure 11. Freundlich plot of HDTMA-VMT$_{0.2M}$.

Table 2. Fluoride adsorption capacity of various adsorbents in literature.

Adsorbent	Adsorption Capacity (mg/g)	References
Magnesium Titanate	0.03	[38]
Granula acid treated bentonite	0.094	[39]
Pumice	0.31	[40]
Zeolite	0.47	[41]
Regenerated spent bleach earth	0.6	[42]
Fe/Zr-Alginate microparticles	0.981	[43]
Gypsiferous limestone	1.07	[44]
Synthetic Siderite	1.77	[45]
Hydrous bismuth oxide	0.06–1.93	[46]
Iron impregnated granular ceramic	1.70–2.16	[47]
Fe-Al-Ce nanocomposite	2.22	[48]
CMPNS	2.3	[49]
Stilbite zeolite modified Fe^{3+}	2.31	[50]
HDTMA-VMT$_{0.2M}$	2.36	Present study

Also, in comparison with other adsorption methods (such as the use of alumina), vermiculite is a naturally occurring clay mineral whereas alumina has to be purchased commercially, making it more expensive than vermiculite. Application of biosorbents in an adsorption method is also generally limited by the water-soluble components of the biosorbent which could dissolve in water and reduce its potability, while pH and temperature variation could also further denaturise the biosorbent [51,52]. Thus vermiculite is less complex in a defluoridation application.

3.6. Adsorption Kinetics

Two major models are used in the study of adsorption kinetics: pseudo-first-order and pseudo-second-order kinetic models. Both models are expressed in Equations (7) and (8).

$$\log(q_e - q_t) = \log q_e - \frac{K_1 t}{2.303} \quad (7)$$

$$\frac{t}{q_t} = \frac{1}{K_2 q_e{}^2} + \frac{t}{q_e} \quad (8)$$

where q_e and q_t are the amounts of adsorbate adsorbed at equilibrium and time "t" (mg/g), K_1 and K_2 are the pseudo-first-order and pseudo-second-order rate constants in 1/minute and g/mg min, respectively. A linear plot of log(q_e – q_t) against t (time) for this study, shows a low correlation

coefficient of 0.2335, thus suggesting that the adsorption did not conform to pseudo-first-order model (Figure 12). On the other hand, a plot of t/q_t against t gave a linear plot with a correlation coefficient of 0.9964 (Figure 13). The results showed that the adsorption conformed to pseudo-second-order reaction, which essentially implies that the mechanism of adsorption is chemisorption [53]. The closeness of the calculated q_e (0.2896) to the experimental q_e (0.2950) values for HDTMA-VMT$_{0.2M}$ further confirms that it obeys pseudo-second-order reaction based on the study by Yu et al. [17] (Table 3).

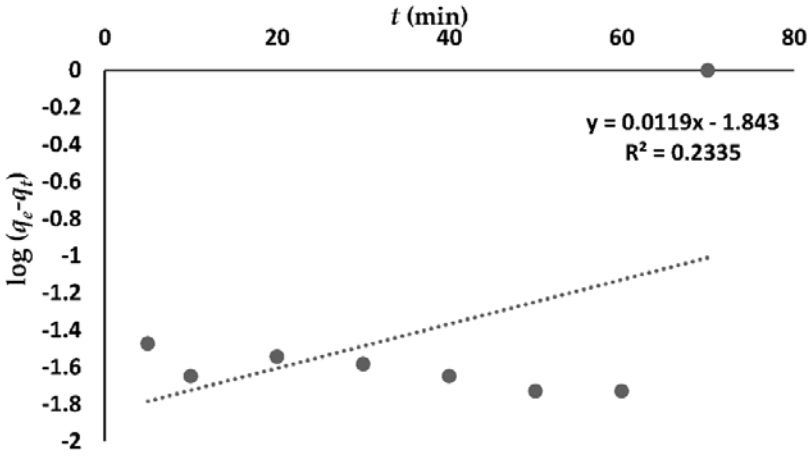

Figure 12. Pseudo-first-order plot of HDTMA-VMT$_{0.2M}$.

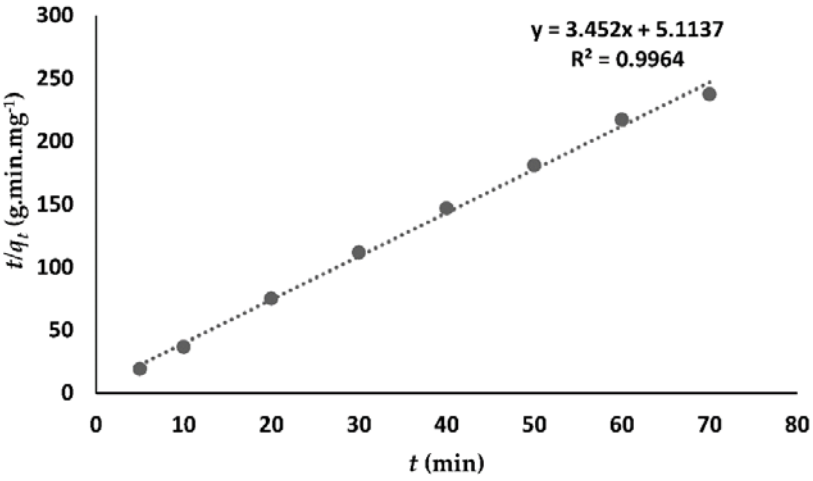

Figure 13. Pseudo-second-order reaction of HDTMA-VMT$_{0.2M}$.

Table 3. Parameters for pseudo-first-order and pseudo-second-order kinetic models.

Adsorbent	q_e exp (mg/g)	Pseudo-First-Order Model			Pseudo-Second-Order Model		
		K_1 ($\times 10^3$ min^{-1})	q_e cal (mg/g)	R^2	K_2 ($\times 10$ g·mg^{-1}·min^{-1})	q_e calc (mg/g)	R^2
HDTMA-VMT$_{0.2M}$	0.2950	0.0274	0.0143	0.0069	0.6757	0.2896	0.9964

The same mechanism was discovered in other anionic adsorption studies such as Senturk et al. [22], Kumar et al. [54], Onyango et al. [20], Yu et al. [17], Wang et al. [28], Asgari et al. [26], Aroke et al. [19], and Slimani et al. [29], amongst others. The formation of a positively charged bilayer on the clay surface was responsible for fluoride attraction [26,55]. Further study by Haggerty [56] also confirms this fact, as it states emphatically that sorption onto positively charged admicelle formation is a major mechanism for anionic component removal by an organomodified adsorbent.

3.7. Mechanism-Based Model

The Weber–Morris model was used to ascertain if intraparticle diffusion was the rate-controlling step of this adsorption using Equation (9).

$$q_t = K_d \sqrt{t} + I \quad (9)$$

where K_d is the intraparticle diffusion rate constant mg/(g/min$^{1/2}$) and I (mg/g) is a constant associated with the thickness of the boundary layer [57]. A plot of q_t against $t^{0.5}$ which passes through the origin indicates intraparticle diffusion as the major rate-controlling step. However, a plot which does not pass through the origin denotes that intraparticle diffusion is not the only rate-controlling step [53]. The intraparticle diffusion plot of this study, as shown in Figure 14, shows a linear plot which deviates from the origin, thus intraparticle diffusion is involved but is not the only mechanism controlling the rate of fluoride adsorption on HDTMA-VMT$_{0.2M}$.

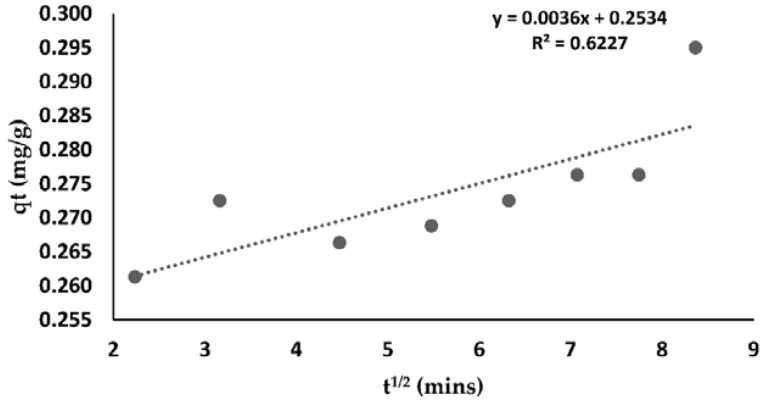

Figure 14. Intraparticle diffusion plot of fluoride on HDTMA-VMT$_{0.2M}$.

4. Conclusions

Fluoride sorption efficiency of vermiculite modified with HDTMA was investigated in this study. The optimised conditions of 2 g adsorbent dosage, 70 min contact time, solution pH of 4, and room temperature (25 °C) guaranteed 51.13% fluoride removal from an 8 mg/L fluoride solution with a maximum adsorption capacity of 2.36 mg/g. This suggests that HDTMA-VMT$_{0.2M}$ can be efficient for fluoride sorption. The adsorption isotherm conformed to both Langmuir and Freundlich isotherms but more to the latter, which indicated that multilayer adsorption took place on the adsorbent. The kinetics obeyed the pseudo-second-order reaction model, which predominantly denotes a case of chemisorption as the mechanism of adsorption while intraparticle diffusion was estimated to be involved in the attraction rate of fluoride onto HDTAM-VMT$_{0.2M}$ surface. The adsorption of fluoride onto HDTMA-VMT$_{0.2M}$ was also attributed to the CH_3 and CH_2 groups introduced to the clay mineral by HDTMABr. This study has shown that vermiculite modified with HDTMABr exhibits fluoride sorption properties, however, further studies should focus on increasing the efficiency of HDTMA-VMT by considering more effective pretreatment procedures as well as other cationic surfactants with higher electropositivity. Efforts should also be made to understand the behaviour of fluoride compounds with change in pH.

Acknowledgments: The authors would like to appreciate the University of Venda, Research and Publications Committee (RPC) for funding this research.

Author Contributions: Tayo Oladipo Ologundudu was responsible for the analysis and writing of the manuscript. John O. Odiyo conceptualised, supervised and controlled the quality of the manuscript while Georges-Ivo E. Ekosse supervised and contributed to the writing of the manuscript.

Conflicts of Interest: The authors declare no conflict of interest.

References

1. Parlikar, A.S.; Mokashi, S.S. Defluoridation of water by moringa oleifera—A natural adsorbent. *Int. J. Eng. Sci. Innov. Technol.* **2013**, *2*, 245–252.
2. World Health Organisation. *Fluoride in Drinking-Water, Background Document for Development of WHO Guidelines for Drinking-Water Quality*; World Health Organization: Geneva, Switzerland, 2004.
3. Kamble, S.P.; Japtap, S.; Labhsetwar, N.K.; Thakare, D.; Godfrey, S.; Devotta, S.; Rayau, S.S. Defluoridation of drinking water using chitin, chitosan and lanthanum modified chitosan. *Chem. Eng. J.* **2007**, *129*, 173–180. [CrossRef]
4. Atia, D.; Hoggui, A. Defluoridation of water by precipitation. *J. Chem. Pharm. Res.* **2012**, *4*, 5180–5184.
5. Patil, S.P.; Ingole, N.W. Studies on defluoridation—A critical review. *J. Eng. Res. Stud.* **2012**, *3*, 111–119.
6. Kumar, N.P.; Kumar, N.S.; Krishnaiah, A. Defluoridation of water using tamarind (*Tamarindus indica*) fruit cover: Kinetics and equilibrium studies. *J. Chil. Chem. Soc.* **2012**, *57*, 1224–1231. [CrossRef]
7. Karthikeyan, M.; Kumar, K.K.; Elango, K.P. Studies on the defluoridation of water using conducting polymer/montmorillonite composites. *Environ. Technol.* **2012**, *33*, 733–739. [CrossRef] [PubMed]
8. Gogoi, P.K.; Baruah, R. Fluoride removal from water by adsorption on acid activated kaolinite clay. *Indian J. Chem. Technol.* **2008**, *15*, 500–503.
9. Sajidu, S.M.I.; Masamba, W.R.L.; Thole, B.; Mwatseteza, J.F. Groundwater fluoride levels in Villages of Southern Malawi and removal studies using bauxite. *Int. J. Phys. Sci.* **2008**, *3*, 1–11.
10. Jain, A.; Singh, S.K. Defluoridation of water using alum impregnated brick powder and its comparison with brick powder. *Int. J. Eng. Sci. Innov. Technol.* **2014**, *3*, 591–596.
11. França, S.C.A.; Arruda, G.M.; Ugarte, J.F.O. Vermiculite utilization on the treatment of water contaminated with organic compounds. In Proceedings of the Enpromer 2005, 2nd Mercosur Congress on Chemical Engineering, Rio de Janeiro, Brazil, 14–18 August 2005.
12. Dizadji, N.; Rashtchi, M.; Dehpouri, S.; Nouri, N. Experimental investigation of adsorption of copper from aqueous solution using vermiculite and clinoptilolite. *Int. J. Environ. Res.* **2013**, *7*, 887–894.
13. Hongo, T.; Yoshino, S.; Yamazaki, A.; Yamasaki, A.; Satokawa, S. Mechanical treatment of vermiculite in vibration milling and its effects on lead (II) adsorption ability. *Appl. Clay Sci.* **2012**, *70*, 74–78. [CrossRef]
14. Ramirez-Valle, V.; Jimenez de Haro, M.C.; Aviles, M.A.; Perez-Maqueda, L.A.; Duran, A.; Pascual, J.; Perez-Rodriguez, J.L. Effect of interlayer cations on high-temperature phases of vermiculite. *J. Therm. Anal. Calorim.* **2006**, *84*, 147–155. [CrossRef]
15. Vazquez, A.; Lopez, M.; Kortaberria, G.; Martin, L.; Mondragon, I. Modification of montmorillonite with cationic surfactant. Thermal and chemical analysis including determination of CEC determination. *Appl. Clay Sci.* **2008**, *41*, 24–36. [CrossRef]
16. Vujakovi, A.; Daković, A.; Lemić, J.; Radosavljević-Mihajlović, A.; Tomašević-Canović, M. Adsorption of inorganic anionic contaminants on surfactant modified minerals. *J. Serbian Chem. Soc.* **2003**, *68*, 833–841. [CrossRef]
17. Yu, X.; Wei, C.; Ke, L.; Hu, Y.; Xie, X.; Wu, H. Development of organovermculite-based adsorbent for the removal of anionic dyes from aqueous solution. *J. Hazard. Mater.* **2010**, *180*, 499–507. [CrossRef] [PubMed]
18. Abate, G.; Masini, J.C. Sorption of atrazine, propazine, deethylatrazine, deisopropylatrazine and hydroxyatrazine onto organovermiculite. *J. Braz. Chem. Soc.* **2005**, *16*, 936–943. [CrossRef]
19. Aroke, U.O.; El-Nafaty, U.A.; Osha, O.A. Removal of oxyanion contaminants from wastewater by sorption onto HDTMA-Br surface modified organo-kaolinite clay. *Int. J. Emerg. Technol. Adv. Eng.* **2014**, *4*, 475–484.
20. Onyango, M.S.; Masukume, M.; Ochieng, A.; Otieno, F. Functionalised natural zeolite and its potential for treating drinking water containing excess amount of nitrate. *Water SA* **2010**, *36*, 655–662. [CrossRef]
21. Ahmed, M.E.I. Cadmium adsorption on HDTMA modified montmorillionite. *J. Eng. Res.* **2009**, *6*, 8–14.
22. Radojevic, M.; Bashkin, V.N. *Practical Environmental Analysis*; The Royal Society of Chemistry: Cambridge, UK, 1999; p. 466.
23. Senturk, H.B.; Ozdes, D.; Gundogdu, A.; Duran, C.; Soylak, M. Removal of phenol from aqueous solutions by adsorption onto organomodified Tirebolu bentonite: Equilibrium, kinetic and thermodynamic study. *J. Hazard. Mater.* **2009**, *172*, 353–362. [CrossRef] [PubMed]
24. Swarnkar, V.; Agrawal, N.; Tomar, R. Sorption of chromate and arsenate by surfactant modified erionite (E-SMZ). *J. Dispers. Sci. Technol.* **2012**, *33*, 919–927. [CrossRef]

25. Li, Z.; Bowman, R.S. Counterion effects on the sorption of cationic surfactant and chromate on natural clinoptilolite. *Environ. Sci. Technol.* **1997**, *31*, 2407–2412. [CrossRef]
26. Asgari, G.; Roshani, B.; Ghanizadeh, G. The investigation of kinetic and isotherm of fluoride adsorption onto functionalize pumice stone. *J. Hazard. Mater.* **2012**, *217–218*, 123–132. [CrossRef] [PubMed]
27. Muiambo, F.H. Inorganic Modification of Palabora Vermiculite. Master's Dissertation, University of Pretoria, Pretoria, South Africa, February 2011.
28. Wang, M.; Liao, L.; Zhang, X.; Li, Z.; Xia, Z.; Cao, W. Adsorption of low-concentration ammonium onto vermiculite from Hebei Province, China. *Clays Clay Miner.* **2011**, *59*, 459–465. [CrossRef]
29. Slimani, M.S.; Ahlafi, H.; Moussout, H.; Chfaira, R.; Zegaoui, O. Evaluation of kinetic and thermodynamic parameters of chromium adsorption on a organobentonite. *Int. J. Adv. Res. Chem. Sci.* **2014**, *1*, 17–29.
30. Dang-I, A.Y.; Boansi, A.O.; Pedevoah, M. Reduction of fluorine in water using clay mixed with hydroxyapatite. *Int. J. Appl. Sci. Technol.* **2015**, *5*, 45–55.
31. Thakre, D.; Rayalu, S.; Kawade, R.; Meshram, S.; Subrt, J.; Labhsetwar, N. Magnesium incorporated bentonite clay for defluoridation of drinking water. *J. Hazard. Mater.* **2010**, *180*, 122–130. [CrossRef] [PubMed]
32. Yilmaz, A.E.; Fil, B.A.; Bayar, S.; Karakaş, Z.K. A new adsorbent for fluoride removal: The utilization of sludge waste from electrocoagulation as adsorbent. *Glob. Nest J.* **2015**, *17*, 186–197.
33. PaliShahjee; Godboley, B.J.; Sudame, A.M. Removal of fluoride from aqueous solution by using low cost adsorbent. *Int. J. Innov. Res. Sci. Eng. Technol.* **2013**, *2*, 2721–2725.
34. Rajkumar, S.; Murugesh, S.; Sivasankar, V.; Darchen, A.; Msagati, T.A.M.; Chaabane, T. Low-cost fluoride adsorbents prepared from a renewable biowaste: Syntheses, characterization and modelling studies. *Arab. J. Chem.* **2015**. [CrossRef]
35. Dada, A.O.; Olalekan, A.P.; Olatunya, A.M.; Dada, O. Langmuir, Freundlich, Temkin and Dubinin–Radushkevich isotherms studies of equilibrium sorption of Zn^{2+} unto phosphoric acid modified rice husk. *J. Appl. Chem.* **2012**, *3*, 38–45.
36. Harikumar, P.S.P.; Jaseela, C.; Megha, T. Defluoridation of water using biosorbents. *Sci. Res.* **2012**, *4*, 245–251. [CrossRef]
37. Achmad, A.; Kassim, J.; Suan, T.K.; Amat, R.C.; Seey, T.L. Equilibrium, kinetic and thermodynamic studies on the adsorption of a direct dye onto a novel green adsorbent developed from *Uncaria gambir* extract. *J. Phys. Sci.* **2012**, *23*, 1–13.
38. Gopal, V.; Elango, K.P. Studies on defluoridation of water using magnesium titanate. *Indian J. Chem. Technol.* **2010**, *17*, 28–33.
39. Ma, Y.; Shi, F.; Zheng, X.; Ma, J.; Gao, C.J. Removal of fluoride from aqueous solution using granular acid-treated bentonite (GHB): Batch and column studies. *J. Hazard. Mater.* **2011**, *185*, 1073–1080. [CrossRef] [PubMed]
40. Malakootian, M.; Moosazadeh, M.; Yousefi, N.; Fatehizadeh, A. Fluoride removal from aqueous solution by pumice: Case study on Kuhbonan water. *Afr. J. Environ. Sci Technol.* **2011**, *5*, 299–306.
41. Gómez-Hortigüela, L.; Pérez-Pariente, J.; García, R.; Chebude, Y.; Díaz, I. Natural zeolites from Ethiopia for elimination of fluoride from drinking water. *Sep. Purif. Technol.* **2013**, *120*, 224–229. [CrossRef]
42. Malakootian, M.; Fatehizadeh, A.; Yousefi, N.; Ahmadian, M.; Moosazadeh, M. Fluoride removal using regenerated spent bleaching earth (RSBE) from groundwater: Case study on Kuhbonan water. *Desalination* **2011**, *277*, 244–249. [CrossRef]
43. Swain, S.K.; Patnaik, T.; Patnaik, P.C.; Jha, U.; Dey, R.K. Development of new alginate entrapped Fe (III)–Zr (IV) binary mixed oxide for removal of fluoride from water bodies. *Chem. Eng. J.* **2013**, *215–216*, 763–771. [CrossRef]
44. Fufa, F.; Alemayehu, E.; Deboch, B. Defluoridation of groundwater using gypsiferous limestone. *J. Environ. Occup. Sci.* **2014**, *3*, 71–76. [CrossRef]
45. Liu, Q.; Guo, H.; Shan, Y. Adsorption of fluoride on synthetic siderite from aqueous solution. *J. Fluor. Chem.* **2010**, *131*, 635–641. [CrossRef]
46. Srivastav, A.L.; Singh, P.K.; Srivastava, V.; Sharma, Y.C. Application of a new adsorbent for fluoride removal from aqueous solutions. *J. Hazard. Mater.* **2013**, *263*, 342–352. [CrossRef] [PubMed]
47. Chen, N.; Zhang, Z.; Feng, C.; Li, M.; Zhu, D.; Sugiura, N. Studies on fluoride adsorption of iron-impregnated granular ceramics from aqueous solution. *Mater. Chem. Phys.* **2011**, *125*, 293–298. [CrossRef]

48. Chen, L.; Wu, H.; Wang, T.; Jin, Y.; Zhang, Y.; Dou, X. Granulation of Fe–Al–Ce nano-adsorbent for fluoride removal from drinking water by spray coating on sand in a fluidized bed. *Powder Technol.* **2009**, *193*, 59–64. [CrossRef]
49. Hernández-Montoya, V.; Ramírez-Montaya, L.A.; Bonilla-Petriciolet, A.; Montes-Morán, M.A. Optimizing the removal of fluoride from water using new carbons obtained by modification of nut shell with a calcium solution from egg shell. *Biochem. Eng. J.* **2012**, *62*, 1–7. [CrossRef]
50. Sun, Y.; Fang, Q.; Dong, J.; Cheng, X.; Xu, J. Removal of fluoride from drinking water by natural stilbite zeolite modified with Fe (III). *Desalination* **2011**, *277*, 121–127. [CrossRef]
51. Rangel-Mendez, J.R.; Barrios, V.A.E.; Davila-Rodriguez, J.L. Chitin Based Biocomposites for Removal of Contaminants from Water: A Case Study of fluoride adsorption. In *Biopolymers*; Elnashar, M., Ed.; InTech: Rijeka, Croatia, 2010; ISBN: 978-953-307-109-1.
52. Mwakabona, H.T.; Said, M.; Machunda, R.L.; Njau, K.N. Plant biomasses for defluoridation appropriateness: Unlocking their potentials. *Res. J. Eng. Appl. Sci.* **2014**, *3*, 167–174.
53. Hameed, B.H.; Mahmoud, D.K.; Ahmad, A.L. Equilibrium modelling and kinetic studies on the adsorption on basic dye by a low cost adsorbent: Coconut (*Cocos nucifera*) bunch waste. *J. Hazard. Mater.* **2008**, *158*, 65–72. [CrossRef] [PubMed]
54. Kumar, P.S.; Vincent, C.; Kirthik, K.; Kumar, K.S. Kinetics and equilibrium studies of Pb^{2+} ion removal from aqueous solutions by use of nano-silversol-coated activated carbon. *Braz. J. Chem. Eng.* **2010**, *27*, 339–346. [CrossRef]
55. Guan, H.; Bestland, E.; Zhu, C.; Zhu, H.; Albertsdottir, D.; Hutson, J.; Simmons, C.T.; Ginic-Markovic, M.; Tao, X.; Ellis, A.V. Variation in performance of surfactant loading and resulting nitrate removal among four selected natural zeolites. *J. Hazard. Mater.* **2010**, *183*, 616–621. [CrossRef] [PubMed]
56. Haggerty, G. Sorption of Inorganic Oxyanions by Organo Zeolite. Master's Thesis, New Mexico Institute of Mining and Technology, Socorro, NM, USA, 1993.
57. Weber, W.J., Jr.; Morris, J.C. Kinetics of adsorption on carbon from solution. *J. Sanit. Eng. Div.* **1963**, *89*, 31–60.